Nonlinear Analysis: Modelling and Control, Vol. 30, No. 4, 747–770
https://doi.org/10.15388/namc.2025.30.42681

Vilnius University Press

Dynamic analysis of a fractional-order rumor spreading model with double time delay under higher-order interactions*

Yang Xia[a], **Haijun Jiang**[a, 1], **Jiarong Li**[a], **Shuzhen Yu**[b]

[a]College of Mathematics and System Sciences,
Xinjiang University, Urumqi 830046, China
jianghaijunxju@163.com; jianghai@xju.edu.cn

[b]College of Mathematics and System Sciences,
Xinjiang Normal University, Urumqi 830046, China

Received: September 4, 2023 / **Revised:** April 22, 2025 / **Published online:** June 27, 2025

Abstract. Although traditional network-based models also explore higher-order interactions, they are limited in capturing the complex impacts of multibody interactions, making it difficult to characterize the reinforcement effect in rumor propagation. With this in mind, firstly, this study introduces the simplicial complexes, a higher-order mathematical tool, to model rumor propagation. Secondly, the fractional-order derivatives are employed to more accurately capture the memory effect and anomalous diffusion phenomenon in the rumor propagation process under higher-order interactions. Then propagation thresholds and the existence of model solutions are investigated. Moreover, the proposed model exhibits bistability, and the Hopf bifurcation is analysed by choosing time delay as the threshold. Numerical simulations suggest that fractional-order rumor spreading models with higher-order interactions are more consistent with actual data than network-based models and integer-order models.

Keywords: rumor spreading, fractional-order model, higher-order interactions, Hopf bifurcation.

1 Introduction

Rumors, a typical type of misinformation, are easy to believe because of their seductive and inflammatory content. Stepping into the new media era, people can spread rumors explosively with the help of online devices, resulting in even worse negative consequences. Dynamic modeling of rumor propagation is an essential method for conducting theoretical research. Through qualitative and quantitative analysis of the proposed model dynamics, we can analyze the process of rumor propagation, reveal rumor patterns, predict trends,

*This research was supported by Xinjiang Key Laboratory of Applied Mathematics (XJDX1401), the National Natural Science Foundation of China (62163035) and Tianchi Talents Introduction Program.

[1]Corresponding author.

explore the causes and critical factors of rumor outbreak and diffusion, and then provide the theoretical basis for prevention and control decisions.

By introducing the compartmental model in infectious diseases into rumor modeling, the classical DK model was proposed [6], pointing the way to the study of rumor dynamics. Drawing on their pioneering work, various novel compartmental models were applied to elucidate the roles played by different groups in rumor spreading such as SEIR [36], SIAR [21], SIQR [14], ILSR [23]. Besides, some individual and social factors are also gradually introduced into rumor modeling such as forgetting mechanism [34], hesitating mechanism [25], self-purification mechanism [30], rumor-refuting mechanism [33], and multilingual environment [24]. But the above models are all integer-order model, which cannot characterize the anomalous spread of rumors, i.e., rumors spread explosively in the early stages and slow down significantly in the later stages. Besides, the memory effect is crucial in rumor spreading as individuals often recall and share previous information, and this affects the pattern of rumor spreading. Note that the fractional-order model cannot only capture abnormal diffusion behaviours and describe more accurately how rumors spread and propagate in social networks, but also reflect the memory effect of the propagation process and provide a better understanding of how past events, historical information, and previous states can affect rumor propagation. Given this, Shu [19] first used fractional-order differential equations to model rumor propagation for studying the memory effect. Some other exploration of fractional-order rumor spreading models are shown in [20, 26, 32]. Furthermore, since the time-sensitive nature of rumors and the lag effect in the transmission process, time delay is also an essential factor in accurately analysing the mechanism of rumour spreading [10, 29]. Time delays are ubiquitous in various systems, significantly affecting their dynamics and stability such as control systems [3, 4], Turing phenomenon [12], and information diffusion [18, 28]. While there is still less literature on exploring the influence of time delay on rumor spreading dynamics using fractional-order models. Combining the real existence of propagation delay and recovery delay, this study will establish a fractional-order rumor propagation model with double time delays to discuss the propagation process in more detail.

Additionally, the above models ignore the topology in the underlying social networks. These models only appropriately portray propagation in small-scale social networks; however, they become infeasible in large-scale interaction networks. With the rise of complex networks, researchers have gradually started to pay attention to the effect of the topological nature of social networks on the propagation process. Zanette [31] first applied complex network theory to the study of rumor propagation by modeling rumor propagation on small-world networks and discovered the existence of rumor propagation queues. Subsequently, Moreno et al. [13] investigated the dynamics of rumor propagation in scale-free networks, comparing computer simulations with conclusions drawn through stochastic analysis methods. Many scholars have studied the propagation dynamics behavior of rumors on complex networks from different perspectives, benefiting from the advantages of complex networks in describing the process of rumor propagation [5, 15, 17].

In fact, the rumor model based on complex networks still has shortcomings in portraying rumor diffusion on social networks, as demonstrated by difficulty in capturing higher-

order interactions, limited ability to handle heterogeneity, difficulty in modeling overlapping communities, inability to capture multiple relationships, and so on. For example, individual is not only influenced by neighboring nodes in the rumor spreading process, but also by neighboring nodes as a whole, which is manifested as the Goebbels effect and the conformity effect [35] in rumor spreading. Noting the advantages of hypergraphs and simplicial complexes in representing higher-order interactions, some scholars have applied them to the modeling of complex systems such as infectious disease transmission [2] and transportation networks [1]. For instance, Jhun et al. established a simplicial SIS model in scale-free uniform hypergraphs, finding that there has a hybrid transition while the strength of hub effect changes in [11]. However, there are few papers that model rumor spreading via higher-order mathematical tools—hypergraphs or simplicial complexes. Thus, it is imperative to further explore the propagation dynamics of rumors under higher-order interactions in depth. Meanwhile, to our knowledge, there is a gap in combining fractional-order and higher-order interactions to analyse rumor propagation dynamics. To that end, under the framework of higher-order interactions, this study will bridge these points by building a simplicial SIRS fractional-order rumor propagation model to explore rumor propagation mechanism. The main contributions of this paper are summarized as follows.

1. A novel rumor spreading model is proposed by applying the modeling methods of fractional derivatives and simplicial complexes, which overcomes the limitations of pairwise interactions and integer-order models in capturing more complex dynamics.
2. The combined effects of propagation and recovery delays are analyzed within a fractional-order rumor propagation model, providing a more comprehensive understanding of the dynamic behavior of rumor spreading.
3. The discovery of the bistable phenomenon induced by higher-order interactions enriches the theoretical research on rumor propagation dynamics.

This paper is in the following organization. The rumor propagation model with higher-order interactions is portrayed in Section 2. In Sections 3.1 and 3.2, the dynamics of delayed-free and delayed systems are discussed, respectively. In Section 4, the feasibility of theoretical results is verified by numerical simulation. In Section 5, the excellence of the proposed model is demonstrated by comparing with a real case. Some conclusions are represented in Section 6.

2 Model instruction

Definition 1. (See [26].) The Caputo's fractional derivative of order α ($0 < \alpha < 1$) of function $g(t) : [t_0, +\infty) \to \mathbb{C}$ is defined by

$$ {}_0^C D_t^\alpha g(t) = \frac{1}{\Gamma(1-\alpha)} \int_{t_0}^{t} \frac{g'(\tau)}{(t-\tau)^\alpha} \, \mathrm{d}\tau, \quad t \geqslant t_0, $$

in which $\Gamma(\cdot)$ is the gamma function.

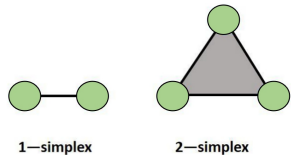

Figure 1. Geometric diagrams of 1-dimensional and 2-dimensional simplex.

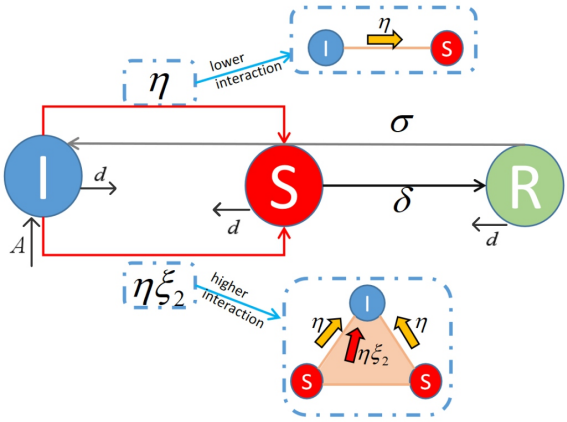

Figure 2. State transition in rumor diffusion with paired and high-order interactions.

According to the classical DK model, we divide the crowd in social networks into three categories, namely I-state, S-state, and R-state, where I-state represents ignorant individuals who have not yet heard the rumor; S-state represents spreaders who know and disseminate the rumor; R-state represents removed individuals who know the rumor but lose interest in spreading it [6].

To better present the description of the rumor propagation process, we first clarify the geometric meaning of the simplex. 1-simplex represents the connected edges between two points, i.e., a connected structure in an ordinary graph, which is a low-order interaction. 2-simplex represents not only the edges between two nodes but also a triangle formed by three nodes together, shown as Fig. 1. We call the interaction between multiple individuals a higher-order interactions. Here we use simplex-based propagation to portray higher-order interactions. Suppose there are three interrelated individuals, one of whom is an ignorant individual, and the other two are spreaders. The probability of the ignorant becoming a spreader increases under the influence of these two spreaders, a situation that can be perfectly described by the 2-simplex, i.e., the higher-order interaction in Fig. 2.

The parameter ξ_1 denotes the strengthening factor based on the 1-simplex propagation. Since the topological structure of 1-simplex propagation is the same as that of pairwise propagation, no additional reinforcement effect is generated. For this reason, we assume that $\xi_1 = 1$. ξ_2 is the strengthening factor based on the 2-simplex propagation. η is the probability of the ignorant individuals becoming the latter after exposure of the ignorant individuals to the spreaders. A and d denote the emigration and migration rates,

respectively. δ is the probability of becoming an removed individual due to one's own loss of interest or after finding out the truth. σ is the probability that the removed individual becomes an ignorant individual again due to forgetting effect. α_{ij} and $\alpha_{ij_1j_2}$ stand for the connection of individuals. If they form a 1-simplex, we have α_{ij}=1, otherwise, α_{ij}=0. If they form a 2-simplex, we have $\alpha_{ij_1j_2}$=1, otherwise, $\alpha_{ij_1j_2}$=0.

We assume that the total number of individuals is N. We regard each individual i ($i = 1, 2, \ldots, N$) as a node and the communication relations among individuals as the edges in the topological structure. Let $I_i(t)$, $S_i(t)$, and $R_i(t)$ represent the probabilities that individual i is in the ignorant state, spreading the rumor, and removed state, respectively, at time t. When a 1-simplex structure is formed between individual i and individual j, that is, $a_{ij} \neq 0$, and if one of them is a rumor spreader and the other is an ignorant individual, then the ignorant individual will turn into a rumor spreader with probability η. If a 2-simplex structure is formed among individual i and j_1, j_2, that is, $a_{ij_1j_2} \neq 0$, and both j_1 and j_2 are rumor spreaders, then the ignorant individual i will be affected by the high-order interaction shown in the dashed box at the bottom of Fig. 2, and thus will turn into a rumor spreader with probability $\eta\ \xi_2$. The Caputo's fractional derivative of order α ($0 < \alpha < 1$) is utilized to capture the memory effect and anomalous diffusion during the rumor propagation process. Specifically, the equations ${}_0^C D_t^\alpha I_i(t)$, ${}_0^C D_t^\alpha S_i(t)$, and ${}_0^C D_t^\alpha R_i(t)$, describe the rate of change of the states of ignorant individuals, spreaders, and removed individuals over time.

Based on the above description and Fig. 2, we can establish a SIRS rumor spreading model from the individual perspective as follows:

$$\begin{aligned}
{}_0^C D_t^\alpha I_i(t) &= A - \eta I_i(t)\left[\xi_1 \sum_{j=1}^{N} \alpha_{ij} S_j(t) + \xi_2 \sum_{j_1,j_2} \alpha_{i,j_1,j_2} S_{j1}(t) S_{j2}(t)\right] \\
&\quad - dI_i(t) + \sigma R_i(t), \\
{}_0^C D_t^\alpha S_i(t) &= \eta I_i(t)\left[\xi_1 \sum_{j=1}^{N} \alpha_{ij} S_j(t) + \xi_2 \sum_{j_1,j_2} \alpha_{i,j_1,j_2} S_{j1}(t) S_{j2}(t)\right] \\
&\quad - dS_i(t) - \delta S_i(t), \\
{}_0^C D_t^\alpha R_i(t) &= \delta S_i(t) - dR_i(t) - \sigma R_i(t)
\end{aligned} \tag{1}$$

with the initial conditions $I_i(0) \geqslant 0$, $S_i(0) \geqslant 0$, $R_i(0) \geqslant 0$, $i = 1, 2, \ldots, N$.

Remark 1. Note that when $\xi_2 = 0$, rumors can only spread through the connecting edge between two nodes in the social network. Therefore, model (1) is an extension of the previous model based on simple graphs. In this paper, ξ_2, as the enhancement factor, should take a value greater than one to fit the realistic context.

Model (1) can help us to understand the based-simplex rumor propagation form in the framework of the proposed model. Nextly, we assume that every individual in the system interacts uniformly with all other individuals. Under this assumption, the specific connection details between individuals can be ignored, and the dynamics of the system can

be described by the average connection strength. Therefore, $\langle k\rangle$ and $\langle k_\Delta\rangle$ representing the global average connection states replace the specific connection parameters α_{ij} and $\alpha_{ij_1j_2}$, respectively. $\langle k_\Delta\rangle$ is the number of triangles formed by each individual through 2-simplex on average, $\langle k\rangle$ is the average degree in complex networks. Then the following mean-field model can be obtained:

$$\begin{aligned}
&{}_0^C D_t^\alpha I(t) = A - \eta I(t)\big[\langle k\rangle S(t) + \xi_2\langle k_\Delta\rangle S^2(t)\big] - dI(t) + \sigma R(t),\\
&{}_0^C D_t^\alpha S(t) = \eta I(t)\big[\langle k\rangle S(t) + \xi_2\langle k_\Delta\rangle S^2(t)\big] - dS(t) - \delta S(t),\\
&{}_0^C D_t^\alpha R(t) = \delta S(t) - dR(t) - \sigma R(t).
\end{aligned} \tag{2}$$

Remark 2. Compared with reference [22] that only takes into account the propagation delay in higher-order rumor spreading, this research innovatively incorporates both the propagation delay and the recovery delay into the higher-order rumor propagation model. This improvement is of great significance because it can more precisely mirror the real situation. Specifically, the model captures both the time delay from receiving to spreading rumor and the time for spreaders to lose interest or change behavior, thus allowing for a more comprehensive grasp of the rumor propagation dynamics.

Remark 3. There already exist some fractional-order rumor models [19, 20, 26, 32]. However, these models omit the time-delay effects in the process of rumor spreading. In this paper, model (2) considers the impact of both propagation delay and recovery delay on rumor diffusion, making the model more in line with real-world propagation scenarios.

3 Theoretical analysis

In this section, we will attend to the dynamical behavior of model (2). Obviously, model (2) is equivalent to the following system by decoupling I-state:

$$\begin{aligned}
&{}_0^C D_t^\alpha S(t) = \eta\big(1 - S(t) - R(t)\big)\big[\langle k\rangle S(t) + \xi_2\langle k_\Delta\rangle S(t)^2\big] - dS(t) - \delta S(t),\\
&{}_0^C D_t^\alpha R(t) = \delta S(t) - dR(t) - \sigma R(t).
\end{aligned} \tag{3}$$

Firstly, we give propagation thresholds as well as discuss the existence of equilibrium of model (3). Apparently, model (3) has a rumor-free equilibrium $E_0 = (S_0, R_0) = (0, 0)$. Then $R_0 = \eta\langle k\rangle/(\delta + d)$ can be acquired by the next generation matrix method [8].

Remark 4.

$$\begin{aligned}
R_0 = \frac{\eta\langle k\rangle}{\delta + d} < 1 \quad &\Longleftrightarrow \quad \eta < \eta_c = \frac{\delta + d}{\langle k\rangle};\\
R_0 \geqslant 1 \quad &\Longleftrightarrow \quad \eta \geqslant \eta_c.
\end{aligned}$$

We are concerned about the existence of the rumor-prevailing equilibrium $E^* = (S^*, R^*)$ of model (3), which is equivalent to whether the following equation has positive solutions in the interval $(0, \min(1,\ (d + \sigma)/\delta)]$:

$$h(S^*) = M_1 S^{*2} + M_2 S^* + M_3 = 0, \tag{4}$$

where

$$M_1 = \eta\xi_2\langle k_\Delta\rangle(\delta + d + \sigma),$$
$$M_2 = \eta\langle k\rangle(\delta + d + \sigma) - (d + \sigma)\eta\xi_2\langle k_\Delta\rangle,$$
$$M_3 = \big[(\delta + d) - \eta\langle k\rangle\big](d + \sigma).$$

Define the two positive solutions of Eq. (4) as $S_1^* = (-M_2 + \sqrt{\Delta})/(2M_1)$ and $S_2^* = (-M_2 - \sqrt{\Delta})/(2M_1)$ when $\Delta > 0$. It is obvious that Eq. (4) has a positive solution S_1^* when $\eta > \eta^c$. We invert ξ_2 by $\Delta = (M_2)^2 - 4M_1M_3 = 0$ and bring η^c to obtain a new propagation threshold $\xi_2^c = (\delta + d + \sigma)\langle k\rangle/((d + \sigma)\langle k_\Delta\rangle)$. Thus, for $\xi_2 \leqslant \xi_2^c$, Eq. (4) does not have a positive solution if $\eta < \eta^c$. Then we analyze the situation where $\xi_2 > \xi_2^c$. To this end, we have the another propagation threshold $\eta^0 = 4\xi_2\langle k_\Delta\rangle(d + \sigma)(\delta + d)(d + \delta + \sigma)/([\langle k\rangle(d + \sigma + \delta) + \xi_2\langle k_\Delta\rangle(d + \sigma)]^2)$ from $\Delta = 0$ when $\xi_2 > \xi_2^c$. According to the expressions of η^0 and η^c, we can easily derive $\eta^0 < \eta^c$ in a situation where $\xi_2 > \xi_2^c$. Moreover, we have the following equivalent expressions in that case:

$$\eta^0 < \eta < \eta^c \iff \Delta > 0;$$
$$\eta = \eta^0 \iff \Delta = 0;$$
$$0 < \eta < \eta^0 \iff \Delta < 0.$$

Hence, it can be obtained that model (3) admits two rumor-prevailing equilibria $E_1^* = (S_1^*, \delta/(d + \sigma)S_1^*)$ and $E_2^* = (S_2^*, \delta/(d + \sigma)S_2^*)$ if $\eta^0 < \eta < \eta^c$, where $E_1^* = E_2^*$ if $\eta = \eta^0$.

3.1 Dynamics of delayed-free system

Next, we will provide the stability of the delayed-free system to set the stage for discussing the effect of time delays on the stability of the system.

Theorem 1. *The rumor-free equilibrium E^0 is locally asymptotically stable when $R_0 < 1$ and unstable when $R_0 > 1$.*

Proof. We calculate the Jacobian matrix of model (3) at E^0 and then derive its characteristic equation as $(\lambda^\alpha + d + \sigma)[\lambda^\alpha - (\eta\langle k\rangle - (\delta + d))] = 0$. Clearly, both eigenvalues satisfy $|\arg(\lambda_i)| > \pi/2 > \alpha\pi/2$ $(i = 1, 2)$ if $\eta < \eta^c$. Thus, the rumor-free equilibrium E^0 is locally asymptotically stable if $R_0 < 1$ based on the Routh–Hurwitz criteria. Similarly, E^0 is unstable if $R_0 > 1$. □

Theorem 2. *The rumor-prevailing equilibrium $E_1^* = (S_1^*, \delta/(d + \sigma)S_1^*)$ is locally asymptotically stable when $R_0 > 1$ and $(\eta\delta\langle k\rangle)^2 < 4\eta\xi_2\langle k_\Delta\rangle(d + \sigma)^2(\eta\langle k\rangle + \sigma - \delta)$. The rumor-prevailing equilibrium $E_2^* = (S_2^*, \delta/(d + \sigma)S_2^*)$ is never stable.*

Proof. First, the Jacobian matrix of model (2) at E_1^* is

$$J(E_1^*) = \begin{pmatrix} -\eta\langle k\rangle S_1^* + \eta\langle k_\Delta\rangle\xi_2 S_1^*(1 - 2S_1^* - \frac{\delta}{d+\sigma}S_1^*) & -\eta\langle k\rangle S_1^* - \eta\langle k_\Delta\rangle\xi_2 S_1^{*2} \\ \delta & -(d + \sigma) \end{pmatrix}.$$

Accordingly, we have

$$\det\big(J(E_1^*)\big) = \frac{\sqrt{M_2^2 - 4M_1M_3}(\sqrt{M_2^2 - 4M_1M_3} - M_2)}{2M_1}$$

and

$$\operatorname{tr}\big(J(E_1^*)\big) = -\eta\xi_2\langle k_\Delta\rangle(S_1^*)^2 + \eta\langle k\rangle\frac{\delta}{d+\sigma}S_1^* + \big(\delta - \sigma - \eta\langle k\rangle\big) \triangleq g(S_1^*).$$

It is possible to conclude that $\det(J(E_1^*)) > 0$ according to $\eta > \eta^c$. Besides, we can get $\operatorname{tr}(J(E_1^*)) < 0$ by the assumption $(\eta\delta\langle k\rangle)^2 - 4\eta\xi_2\langle k_\Delta\rangle(d+\sigma)^2(\eta\langle k\rangle + \sigma - \delta) < 0$. Therefore, the rumor-prevailing equilibrium E_1^* is locally asymptotically stable for $\eta > \eta^c$, that is, $R_0 > 1$ when the assumption is hold.

Likewise, we can get $\det(J(E_2^*))$ and $J(E_2^*)$. Following from the existence condition of rumor-prevailing equilibrium E_2^*, that is, $\xi_2 > \xi_2^c$ and $\eta^0 < \eta < \eta^c$, we can draw that $0 < \sqrt{\Delta} < -M_2$. Thus, we have $\det(J(E_2^*)) < 0$, suggesting that model (3) has positive roots, i.e., E_2^* is never stable. □

Remark 5. From Theorems 1 and 2, the higher-order interactions have no effect on the stability of the rumor-free equilibrium, but make a difference in the stability of the rumor-prevailing equilibrium.

Remark 6. It can be inferred that model (2) will exhibit a bistable state when $\eta \in [\eta^0, \eta^c]$.

3.2 Dynamics of delayed system

Influenced by various real-world factors, individuals cannot spread rumors immediately after acquiring spreadability, and it takes time for spreaders to verify the information after gaining debunking information, leading them not to stop spreading rumors immediately either, so it is reasonable to introduce propagation time delay and recovery time delay into model (2). τ^1 represents the time lag between an individual becoming aware of the rumor and starting to spread it. In real life, when people receive information, they may need time to verify and understand it before deciding to spread it. The recovery time delay τ^2 refers to the time it takes for a spreader to stop spreading the rumor after realizing its inaccuracy or losing interest. This could be due to the spreader finding reliable refuting information or simply forgetting about the rumor. Then we get the following delayed rumor spreading model:

$$\begin{aligned}
{}_0^C D_t^\alpha I(t) &= A - \eta I\big(t-\tau^1\big)\big[\langle k\rangle S\big(t-\tau^1\big) + \xi_2\langle k_\Delta\rangle S\big(t-\tau^1\big)^2\big] \\
&\quad - dI(t) + \sigma R(t), \\
{}_0^C D_t^\alpha S(t) &= \eta I\big(t-\tau^1\big)\big[\langle k\rangle S\big(t-\tau^1\big) + \xi_2\langle k_\Delta\rangle S\big(t-\tau^1\big)^2\big] \\
&\quad - dS(t) - \delta S(t-\tau^2), \\
{}_0^C D_t^\alpha R(t) &= \delta S\big(t-\tau^2\big) - dR(t) - \sigma R(t).
\end{aligned} \tag{5}$$

Noting that the rumor-prevailing equilibrium E_2^* is always unstable, thus we should consider only the effect of time delay on the rumor-prevailing equilibrium E_1^*. In this

section, we select the propagation time delay τ^1 and the recovery time delay τ^2 as bifurcation parameters. The bifurcation result caused by time delay is divided into four cases to discuss, which will be elaborated separately by the following four theorems.

We provide two symbols for the description of the following theorem:

$$B_2^2 = \big[(d+\delta)(d+\sigma)\big]^2$$

and

$$B_4^2 = (S_1^*)^2\bigg\{(d+\sigma)\bigg[\eta\langle k\rangle - \eta\langle k_\Delta\rangle\xi_2\bigg(1-2S_1^* - \frac{\delta}{d+\sigma}S_1^*\bigg)\bigg] + \delta\big(\eta\langle k\rangle + \eta\langle k_\Delta\rangle\xi_2 S_1^*\big)\bigg\}^2.$$

Theorem 3. *If $\tau^1 > 0$, $\tau^2 = 0$, and $(B_2)^2 < (B_4)^2$, the rumor-prevailing equilibrium E_1^* is locally asymptotically stable when $\tau^1 \in [0, \tau_{01}^1)$ and unstable when $\tau^1 > \tau_{01}^1$. Model* (5) *with*

$$\tau^1 = \tau_{01}^1 = \min_{k=0,1,\dots}\bigg\{\frac{1}{w_1}\bigg[\arccos\bigg(\frac{-C_1C_3 - C_2C_4}{C_1^2 + C_2^2}\bigg) + 2k\pi\bigg]\bigg\}$$

undergoes a Hopf bifurcation at the rumor-prevailing equilibrium point E_1^*.

Proof. For this purpose, we calculate the Jacobian matrix at the rumor-prevailing equilibrium point E_1^*:

$$J_1(E_1^*) = \begin{pmatrix} [-\eta\langle k\rangle + \eta\langle k_\Delta\rangle\xi_2(1-2S_1^* - \frac{\delta}{d+\sigma}S_1^*)]S_1^*\mathrm{e}^{-s\tau^1} - (d+\delta) & QS_1^*\mathrm{e}^{-s\tau^1} \\ \delta & -(d+\sigma) \end{pmatrix},$$

where $Q = -(\eta\langle k\rangle + \eta\langle k_\Delta\rangle\xi_2 S_1^*)$. This yields the following characteristic equation:

$$s^{2\alpha} + B_1 s^\alpha + B_2 + B_3 s^\alpha \mathrm{e}^{-s\tau^1} + B_4\mathrm{e}^{-s\tau^1} = 0, \tag{6}$$

where

$$\begin{aligned} B_1 &= 2d + \delta + \sigma, \qquad B_2 = (d+\delta)(d+\sigma), \\ B_3 &= \bigg[\eta\langle k\rangle - \eta\langle k_\Delta\rangle\xi_2\bigg(1-2S_1^* - \frac{\delta}{d+\sigma}S_1^*\bigg)\bigg]S_1^* - d - \delta, \\ B_4 &= S_1^*(d+\sigma)\bigg[\eta\langle k\rangle - \eta\langle k_\Delta\rangle\xi_2\bigg(1-2S_1^* - \frac{\delta}{d+\sigma}S_1^*\bigg)\bigg] \\ &\quad + \delta\big(\eta\langle k\rangle + \eta\langle k_\Delta\rangle\xi_2 S_1^*\big)S_1^*. \end{aligned}$$

Suppose that Eq. (6) has a pure imaginary root $s = \mathrm{i}w_1$ and $w_1 > 0$, it follows that

$$(\mathrm{i}w_1)^{2\alpha} + B_1(\mathrm{i}w_1)^\alpha + B_2 + B_3(\mathrm{i}w_1)^\alpha\mathrm{e}^{-\mathrm{i}w_1\tau^1} + B_4\mathrm{e}^{-\mathrm{i}w_1\tau^1} = 0.$$

Then separating the real and imaginary parts yields

$$\begin{aligned}&\left(B_3w_1^\alpha\cos\frac{\alpha\pi}{2}+B_4\right)\cos\tau^1w_1+B_3w_1^\alpha\sin\frac{\alpha\pi}{2}\sin\tau^1w_1\\&\quad=B_2+B_1w_1^\alpha\cos\frac{\alpha\pi}{2}+w_1^{2\alpha}\cos\alpha\pi,\\&B_3w_1^\alpha\sin\frac{\alpha\pi}{2}\cos\tau^1w_1-\left(B_3w_1^\alpha\cos\frac{\alpha\pi}{2}+B_4\right)\sin\tau^1w_1\\&\quad=w_1^{2\alpha}\sin\alpha\pi+B_1w_1^\alpha\sin\frac{\alpha\pi}{2}.\end{aligned}$$

Let

$$\begin{aligned}C_1&=\left(B_3w_1^\alpha\cos\frac{\alpha\pi}{2}+B_4\right)\cos\tau^1w_1,\\C_2&=B_3w_1^\alpha\sin\frac{\alpha\pi}{2},\\C_3&=w_1^{2\alpha}\cos\alpha\pi+B_1w_1^\alpha\cos\frac{\alpha\pi}{2}+B_2,\\C_4&=w_1^{2\alpha}\sin\alpha\pi+B_1w_1^\alpha\sin\frac{\alpha\pi}{2}.\end{aligned}$$

Thus, we have $\sin\tau_1w_1=(C_1C_4-C_2C_3)/(C_1^2+C_2^2)$, $\cos\tau_1w_1=(-C_1C_3-C_2C_4)/(C_1^2+C_2^2)$. According to $\sin^2w_1\tau^1+\cos^2w_1\tau^1=1$, we can see that there is a positive real root w_1 if $B_2^2<B_4^2$. Then the bifurcation point can be expressed as

$$\tau_{01}^1=\min_{k=0,1,\dots}\left\{\tau_k^1\right\}=\min_{k=0,1,\dots}\left\{\frac{1}{w_1}\left[\arccos\frac{-C_1C_3-C_2C_4}{C_1^2+C_2^2}+2k\pi\right]\right\}.$$

Next, by taking the derivative of τ_1 on both sides of Eq. (6), we obtain

$$\left.\frac{\mathrm{d}s}{\mathrm{d}\tau^1}\right|_{s=\mathrm{i}w_1,\,\tau^1=\tau_{01}^1}=\frac{E_1+\mathrm{i}E_2}{F_1+\mathrm{i}F_2},$$

where

$$\begin{aligned}E_1&=w_1\left[B_4\sin w_1\tau_0^1+B_3w_1^\alpha\sin\left(w_1\tau_0^1-\frac{\alpha\pi}{2}\right)\right],\\E_2&=w_1\left[B_4\cos w_1\tau_0^1+B_3w_1^\alpha\cos\left(w_1\tau_0^1-\frac{\alpha\pi}{2}\right)\right],\\F_1&=w_1^\alpha\left[2\alpha w_1^{\alpha-1}\sin\alpha\pi+\alpha B_1w_1^{-1}\sin\frac{\alpha\pi}{2}+\alpha B_3w_1^{-1}\sin\frac{\alpha\pi}{2}-w_1\tau_0^1\right.\\&\quad\left.-B_3w_1^{-1}\tau_0^1\cos\left(\frac{\alpha\pi}{2}-w_1\tau_0^1\right)\right]-B_4\tau_0^1\cos w_1\tau_0^1,\\F_2&=w_1^\alpha\left[2\alpha w_1^{\alpha-1}\cos\alpha\pi+\alpha B_1w_1^{-1}\cos\frac{\alpha\pi}{2}+\alpha B_3w_1^{-1}\cos\left(\frac{\alpha\pi}{2}-w_1\tau_0^1\right)\right.\\&\quad\left.-B_3w_1^{-1}\tau_0^1\sin\left(\frac{\alpha\pi}{2}-w_1\tau_0^1\right)\right]-B_4\tau_0^1\sin w_1\tau_0^1.\end{aligned}$$

Then we have $\mathrm{Re}(\mathrm{d}s/\mathrm{d}\tau^1|_{\tau^1=\tau_{01}^1,\, w=w_1}) = (E_1F_1 + E_2F_2)/(F_2^2 + F_1^2) \neq 0$ under the condition $E_1F_1 + E_2F_2 > 0$, which suggests that a Hopf bifurcation will occur at $\tau_1 = \tau_{01}^1$, $w = w_1$. □

Theorem 4. *If $\tau^1 = 0$, the rumor-prevailing equilibrium E_1^* is locally asymptotically stable when $\tau^2 \in (0, \tau_{01}^2)$ and unstable when $\tau^2 > \tau_{01}^2$. Model* (5) *undergoes a Hopf bifurcation at the rumor-prevailing equilibrium point E_1^* when*

$$\tau^2 = \tau_{01}^2 = \min_{k=0,1,\ldots}\{\tau_k^2\} = \min_{k=0,1,\ldots}\left\{\frac{1}{w_2}\left[\arccos\frac{-D_1D_3 - D_2D_4}{D_1^2 + D_2^2} + 2k\pi\right]\right\},$$

where

$$\begin{aligned}
D_1 &= w_2^{2\alpha}\cos(\alpha\pi) - (B_1 + B_4)w^\alpha\cos\frac{\alpha\pi}{2} + B_2B_4,\\
D_2 &= \sin(\alpha\pi)w_2^{2\alpha} - w^\alpha(B_1 + B_4)\sin\frac{\alpha\pi}{2},\\
D_3 &= w_2^\alpha B_2\cos\frac{\alpha\pi}{2} - B_2(B_4 - B_3), \qquad D_4 = w^\alpha B_2\sin\frac{\alpha\pi}{2}.
\end{aligned}$$

Proof. The proof is similar to that of Theorem 3 and is therefore omitted. □

Theorem 5. *If $\tau^1 \in T_1^* = \{\tau^1 = \widetilde{\tau}^1,\, 0 < \widetilde{\tau}^1 < \tau_{01}^1\}$, the rumor-prevailing equilibrium E_1^* is locally asymptotically stable when $0 < \tau^2 < \tau_{02}^2$ and unstable when $\tau^2 > \tau_{02}^2$. Model* (5) *undergoes a Hopf bifurcation at the rumor-prevailing equilibrium point E_1^* when*

$$\tau^2 = \tau_{02}^2 = \min_{k=0,1,\ldots}\left\{\frac{1}{w_3}\left[\arccos\frac{-L_1L_3 - L_2L_4}{L_1^2 + L_2^2} + 2k\pi\right]\right\}.$$

Proof. Analogously, we get the characteristic equation at E_1^* for this case as

$$s^{2\alpha} + H_1s^\alpha + H_2\mathrm{e}^{-s\widetilde{\tau}^1} + H_3\mathrm{e}^{-s\tau^2} + H_4\mathrm{e}^{-s\widetilde{\tau}^1}\mathrm{e}^{-s\tau^2} = 0, \tag{7}$$

where $H_1 = 2d + \sigma$, $H_2 = (d + \sigma + s^\alpha)B_3$, $H_3 = \delta(d + \sigma + s^\alpha)$, $H_4 = B_5 = \delta(\eta\langle k\rangle + \eta\langle k_\Delta\rangle\xi_2S_1^*)S_1^*$. Suppose that Eq. (7) has a pure imaginary root $s = \mathrm{i}w_3$ and $w_3 > 0$, then

$$\begin{aligned}
&(\mathrm{i}w_3)^{2\alpha} + H_1(\mathrm{i}w_3)^\alpha + \left(d + \sigma + (\mathrm{i}w_3)^\alpha\right)\left[\mathrm{e}^{-\mathrm{i}w_3\widetilde{\tau}^1} + \delta\mathrm{e}^{-\mathrm{i}w_3\tau^2}\right]\\
&\quad + H_4\mathrm{e}^{-\mathrm{i}w_3\widetilde{\tau}^1}\mathrm{e}^{-\mathrm{i}w_3\tau^2} = 0.
\end{aligned}$$

Separating the real and imaginary parts, we get

$$\begin{aligned}
L_1\cos\tau^2w_3 + L_2\sin\tau^2w_3 &= -L_3,\\
L_2\cos\tau^2w_3 - L_1\sin\tau^2w_3 &= -L_4,
\end{aligned}$$

where

$$\begin{aligned}
L_1 &= \delta B_5\cos w_3\widetilde{\tau}^1 + w_4^\alpha\delta\cos\frac{\alpha\pi}{2} + \delta(d + \sigma),\\
L_2 &= w_4^\alpha\delta\sin\frac{\alpha\pi}{2} - \delta B_5\sin w_4\widetilde{\tau}^1,
\end{aligned}$$

$$L_3 = w_3^{2\alpha}\cos\alpha\pi + w_3^{\alpha}(2d+\sigma)\cos\frac{\alpha\pi}{2} + \cos w_3\widetilde{\tau}^1 B_3\left[w_3^{\alpha}\cos\frac{\alpha\pi}{2} + (d+\sigma)\right] + B_3 w_3^{\alpha}\sin\frac{\alpha\pi}{2}\sin w_3\widetilde{\tau}^1,$$

$$L_4 = w_3^{2\alpha}\sin\alpha\pi + w_3^{\alpha}(2d+\sigma)\sin\frac{\alpha\pi}{2} - \sin w_3\widetilde{\tau}^1 B_3\left[w_3^{\alpha}\cos\frac{\alpha\pi}{2} - (d+\sigma)\right] + B_3 w_3^{\alpha}\sin\frac{\alpha\pi}{2}\cos w_3\widetilde{\tau}^1.$$

Hence, $\sin\tau^2 w_3 = (L_1L_4 - L_2L_3)/(L_1^2 + L_2^2)$ and $\cos\tau^2 w_3 = (-L_1L_3 - L_2L_4)/(L_1^2 + L_2^2)$.

From Eq. (7), we obtain

$$\left.\frac{\mathrm{d}s}{\mathrm{d}\tau^2}\right|_{w=w_3,\,\tau^2=\tau_{01}^2} = \frac{M_1 + \mathrm{i}M_2}{M_3 + \mathrm{i}M_4},$$

where

$$M_1 = \delta w_3^{\alpha+1}\sin\left(w_3\tau_{02}^2 - \frac{\alpha\pi}{2}\right) + w_3\delta(d+\sigma)\sin w_3\tau_{02}^2 + w_3B_5\sin\bigl(w_3\tau_{02}^2 + w_3\widetilde{\tau}^1\bigr),$$

$$M_2 = \delta w_3^{\alpha+1}\cos\left(w_3\tau_{02}^2 - \frac{\alpha\pi}{2}\right) + w_3\delta(d+\sigma)\cos w_3\tau_{02}^2 + w_3B_5\cos\bigl(w_3\tau_{02}^2 + w_3\widetilde{\tau}^1\bigr),$$

$$\begin{aligned} M_3 = {} & 2\alpha w_3^{2\alpha-1}\sin\alpha\pi + (2d+\sigma)\alpha w_3^{\alpha-1}\sin\frac{\alpha\pi}{2} \\ & + \cos w_3\widetilde{\tau}^1\left[-\widetilde{\tau}^1 B_3 w_3^{\alpha}\cos\frac{\alpha\pi}{2} - (d+\sigma)\widetilde{\tau}^1 B_3 + B_3\alpha\sin\frac{\alpha\pi}{2}\right] \\ & - \sin\widetilde{\tau}^1\left[\widetilde{\tau}^1 B_3 w^{\alpha}\sin\frac{\alpha\pi}{2} + B_3\alpha\cos\frac{\alpha\pi}{2}\right] - \tau_{02}^2\delta(d+\sigma)\cos w_3\tau_{02}^2 \\ & - \tau_{02}^2\delta w_3^{\alpha}\cos\left(w_3\tau_{02}^2 - \frac{\alpha\pi}{2}\right) + \delta\alpha\sin\left(\frac{\alpha\pi}{2} - w_3\tau_{02}^2\right) \\ & - \bigl(\widetilde{\tau}^1 + \tau_{02}^2\bigr)B_5\cos\bigl(w_3\tau_{02}^2 + w_3\widetilde{\tau}^1\bigr), \end{aligned}$$

$$\begin{aligned} M_4 = {} & -2\alpha w_3^{2\alpha-1}\cos\alpha\pi - (2d+\sigma)\alpha w_3^{\alpha-1}\cos\frac{\alpha\pi}{2} \\ & + \sin w_3\widetilde{\tau}^1\left[\widetilde{\tau}^1 B_3 w_3^{\alpha}\cos\frac{\alpha\pi}{2} + (d+\sigma)\widetilde{\tau}^1 B_3 - B_3\alpha\sin\frac{\alpha\pi}{2}\right] \\ & - \cos\widetilde{\tau}^1\left[\widetilde{\tau}^1 B_3 w^{\alpha}\sin\frac{\alpha\pi}{2} + B_3\alpha\cos\frac{\alpha\pi}{2}\right] + \tau_{02}^2\delta(d+\sigma)\sin w_3\tau_{02}^2 \\ & + \tau_{02}^2\delta w_3^{\alpha}\sin\left(w_3\tau_{02}^2 - \frac{\alpha\pi}{2}\right) - \delta\alpha\cos\left(\frac{\alpha\pi}{2} - w_3\tau_{02}^2\right) \\ & + \bigl(\widetilde{\tau}^1 + \tau_{02}^2\bigr)B_5\sin\bigl(w_3\tau_{02}^2 + w_3\widetilde{\tau}^1\bigr). \end{aligned}$$

In order to get the conditions of the Hopf bifurcation, we suppose $(M_1M_3 + M_2M_4)/(M_3^2 + M_4^2) \neq 0$. Then the transversality condition $\mathrm{Re}(\mathrm{d}s/\mathrm{d}\tau^2|_{\tau=\tau_{02}^2,\,w=w_3}) \neq 0$

holds. Therefore, we can denote $\tau_{02}^2 = \min_{k=0,1,\ldots}\{(1/w_3)[\arccos(-L_1L_3 - L_2L_4)/(L_1^2 + L_2^2) + 2k\pi]\}$. Then Eq. (7) has a purely imaginary root $\mathrm{i}w_3$. Thus, there is a Hopf bifurcation when τ_2 crosses τ_{02}^2. □

Theorem 6. *If $\tau^2 \in T_2^* = \{\tau^2 = \widetilde{\tau}^2,\ 0 < \widetilde{\tau}^2 < \tau_{01}^2\}$, the rumor-prevailing equilibrium E_1^* is locally asymptotically stable when $\tau^1 \in (0, \tau_{02}^1)$ and unstable when $\tau^1 > \tau_{02}^1$. Model* (5) *undergoes a Hopf bifurcation at the rumor-prevailing equilibrium point E_1^* when*

$$\tau^1 = \tau_{02}^1 = \min_{k=0,1,\ldots}\left\{\frac{1}{w_4}\left[\arccos\frac{-P_1P_3 - P_2P_4}{P_1^2 + P_2^2} + 2k\pi\right]\right\},$$

where

$$\begin{aligned}
P_1 &= \delta B_5 \cos w_4\widetilde{\tau}^2 - w_4^\alpha B_3 \cos\frac{\alpha\pi}{2} - \delta(d+\sigma),\\
P_2 &= -w_4^\alpha B_3 \sin\frac{\alpha\pi}{2} - \delta B_5 \sin w_4\widetilde{\tau}^2,\\
P_3 &= w_4^{2\alpha}\cos\alpha\pi + w_4^\alpha \cos\frac{\alpha\pi}{2}(2d+\sigma) + \cos w_4\widetilde{\tau}_2\left[w_4^\alpha\cos\frac{\delta\alpha\pi}{2} + \delta(d+\sigma)\right]\\
&\quad + \delta w^\alpha \sin\frac{\alpha\pi}{2}\sin w_4\widetilde{\tau}^2,\\
P_4 &= w_4^{2\alpha}\sin\alpha\pi + w_4^\alpha \sin\frac{\alpha\pi}{2}(2d+\sigma) - \sin w_4\widetilde{\tau}_2\left[w_4^\alpha\cos\frac{\delta\alpha\pi}{2} - \delta(d+\sigma)\right]\\
&\quad + \delta w^\alpha \sin\frac{\alpha\pi}{2}\cos w_4\widetilde{\tau}^2.
\end{aligned}$$

Proof. Suppose $(\operatorname{Re}Q\operatorname{Re}K + \operatorname{Im}Q\operatorname{Im}K)/(\operatorname{Re}^2K + \operatorname{Im}^2K) \neq 0$, where Q and K are expressed as

$$\begin{aligned}
Q(s) &= B_3 s^{\alpha+1}\mathrm{e}^{-s\tau^1} + B_3(d+\sigma)s\mathrm{e}^{-s\tau^1} + sB_5\mathrm{e}^{-s\tau^1}\mathrm{e}^{-s\widetilde{\tau}^2},\\
K(s) &= 2\alpha s^{2\alpha-1} + (2d+\sigma)\alpha s^{\alpha-1}\\
&\quad - \mathrm{e}^{-s\tau^1}\left[\tau^1 B_3\left(s^\alpha + d + \sigma\right) - \alpha s^{\alpha-1}\right]\\
&\quad + \mathrm{e}^{-s\widetilde{\tau}^2}\left[-\widetilde{\tau}^2\delta\left(s^\alpha + d + \sigma\right) + \delta\alpha s^{\alpha-1}\right]\\
&\quad - \left(\tau^1 + \widetilde{\tau}^2\right)B_5\mathrm{e}^{-s\widetilde{\tau}^2}\mathrm{e}^{-s\tau^1}.
\end{aligned}$$

Then Theorem 6 can be proved by using a similar method as in Theorem 5, and the proof process is omitted here. □

Remark 7. Unlike the rumor propagation model with higher-order interactions in [22], which only identifies a single Hopf bifurcation triggered by time delays, our model detects two Hopf bifurcations triggered by time delays. This indicates that our model can capture more complex dynamic behaviors and bifurcation phenomena in rumor spreading, thereby providing a more comprehensive understanding of the evolution of rumors under the influence of time delays.

Next, we compare the above delay-free system and delayed system in terms of theoretical results, modeling significance and application scenarios to gain a better understanding of the model differences.

Theoretical results. In the delayed-free system, the model focuses on the immediate interactions and transitions among the states of individuals without considering the time lags. This allows for a relatively straightforward analysis of the basic equilibrium and stability conditions, as presented in Theorems 1 and 2. The stability of the rumor-free and rumor-prevailing equilibria can be determined based on the values of parameters such as the basic reproduction number R_0 and certain conditions related to the interaction factors. However, introducing propagation and recovery time delays in the delayed system, the model becomes more complex. The time delays introduce a dynamic element that can change the stability behavior of the equilibria. As demonstrated in Theorems 3–6, the presence of time delays can cause the rumor-prevailing equilibrium E_1^* to change from stable to unstable and trigger Hopf bifurcations under specific conditions. This indicates that the time delays have a significant impact on the long-term behavior and oscillation patterns of the rumor spreading process.

Modeling significance and application scenarios. The delay-free system is crucial for grasping the basic dynamic behavior of the rumor spreading model without time lag effects. It helps clarify the influence of parameters like the basic reproduction number and interaction strength on rumor spreading, providing a simple framework for analyzing equilibrium stability and basic trends through decoupling the I-state and deriving characteristic equations. In contrast, the delayed system better reflects the real world where information dissemination and spreader behavior have time delays. It can explain oscillation and instability in rumor spreading, offering more accurate predictions and a deeper understanding of rumor development trends, thus possessing stronger practical application value in analyzing and forecasting rumor evolution in real social networks.

3.3 Model promotion

In reality, an ignorant individual may have L ($L > 2$) communicators spreading rumors to him or her, and the larger L the more likely the ignorant individual is to be a communicator, which is reflected in the Bandwagon effect and Goebbels effect formed by multiple individuals in communication. Therefore, considering higher-dimensional simplex-based propagation, model (5) can be generalized as

$$\begin{aligned}
{}_0^C D_t^\alpha I(t) &= A - \eta I\big(t-\tau^1\big)\left[\langle k\rangle S\big(t-\tau^1\big) + \xi_l \sum_{l=2}^{L} \langle k_l\rangle S\big(t-\tau^1\big)^l\right] \\
&\quad - dI(t) + \sigma R(t), \\
{}_0^C D_t^\alpha S(t) &= \eta I\big(t-\tau^1\big)\left[\langle k\rangle S\big(t-\tau^1\big) + \xi_l \sum_{l=2}^{L} \langle k_l\rangle S\big(t-\tau^1\big)^l\right] \\
&\quad - dS(t) - \delta S(t-\tau^2), \\
{}_0^C D_t^\alpha R(t) &= \delta S\big(t-\tau^2\big) - dR(t) - \sigma R(t),
\end{aligned}$$

where $\langle k_l \rangle$ is the number of l-dimensional geometric entity formed by each individual through l-simplex on average, ξ_l shows the strengthening effect based on the l-simplex propagation.

Remark 8. Note that the more spread individuals an individual is exposed to, the stronger the enhancement factor should be. Therefore, we assume $\xi_{l_i} \leqslant \xi_{l_j}$ when $l_i < l_j$. In addition, for $\langle k_{l_i} \rangle$ and $\langle k_{l_j} \rangle$, there is no such assumption about $l_i < l_j$ according to the real cases in [9, 16].

Remark 9. The propagation based on l-simplex works if and only if l neighbor nodes of an ignorant individual are all spreaders, however, the probability of this occurrence is small when l is large. Therefore, we will not carry out theoretical analysis here.

4 Numerical simulation

In this section, the validity of the theoretical results and the applicability of the proposed model are confirmed by choosing appropriate parameters for numerical simulation and fitting real cases. We utilized Matlab 2023b for the numerical simulations.

Example 1. Let $\alpha = 0.9$, $A = d = 0.01$, $\xi_2 = 1.59$, $\eta = 0.59$, $\delta = 0.79$, $\sigma = 0.69$, $\langle k_\Delta \rangle = \langle k \rangle = 2$. Then we get $R_0 = 0.725 < 1$. From Fig. 3(a), E_0 is locally asymptotically stable, which is consistent with Theorem 1.

Example 2. Let $\alpha = 0.9$, $A = d = 0.01$, $\xi_2 = 1.59$, $\eta = 0.59$, $\delta = 0.79$, $\sigma = 0.69$, $\langle k_\Delta \rangle = \langle k \rangle = 2$. Then we get $R_0 = 1.475 > 1$ and $(\eta\delta\langle k \rangle)^2 - 4\eta\xi_2\langle k_\Delta \rangle(d+\sigma)^2(\eta\langle k \rangle + \sigma - \delta) \approx -3.1 < 0$. In this case, it can be seen from Fig. 3(b) that E_1^* is locally asymptotically stable.

Remark 10. Note that the stability of the rumor-prevailing equilibrium after adding higher-order interactions no longer depends only on the basic reproduction number R_0 but also requires some additional conditions reflecting higher-order interactions.

Example 3. Let $\alpha = 0.9$, $A = d = 0.01$, $\xi_2 = 3.59$, $\eta = 0.59$, $\delta = 0.79$, $\sigma = 0.99$, $\langle k_\Delta \rangle = \langle k \rangle = 2$, $\tau^2 \equiv 0$. Then we can get $\tau_{01}^1 \approx 5.25$, and the values of τ^1 in Figs. 4(a) and 4(b) are 1.5 and 14, respectively. From Fig. 4(a), we see that the rumor-prevailing equilibrium E_1^* is locally asymptotically stable if $\tau^1 < \tau_{01}^1$ and $\tau^2 = 0$, and from Fig. 4(b), we observe that the rumor-prevailing equilibrium E_1^* is unstable if $\tau^1 > \tau_{01}^1$. Therefore, there exists a Hopf bifurcation when τ^1 pass through τ_{01}^1.

Example 4. Let $\alpha = 0.9$, $A = d = 0.01$, $\xi_2 = 3.59$, $\eta = 0.59$, $\delta = 0.99$, $\sigma = 0.99$, $\langle k_\Delta \rangle = \langle k \rangle = 2$, $\tau^1 \equiv 0$. Then we can get $\tau_{01}^2 \approx 0.68$, and the values of τ^2 in Figs. 5(a) and 5(b) are 0.55 and 0.7, respectively. From Fig. 5(a), we see that the rumor-prevailing equilibrium E_1^* is locally asymptotically stable if $\tau^2 < \tau_{01}^2$ and $\tau^1 = 0$, and from Fig. 5(b), we observe that the rumor-prevailing equilibrium E_1^* is unstable if $\tau^2 > \tau_{01}^2$ and $\tau^1 = 0$. Therefore, there exists a Hopf bifurcation when τ^2 pass through τ_{01}^2. In addition, comparing Figs. 5(a) and 5(b), we can see that the model oscillates more severely in Fig. 5(b), indicating that the model is more sensitive to recovery time delay.

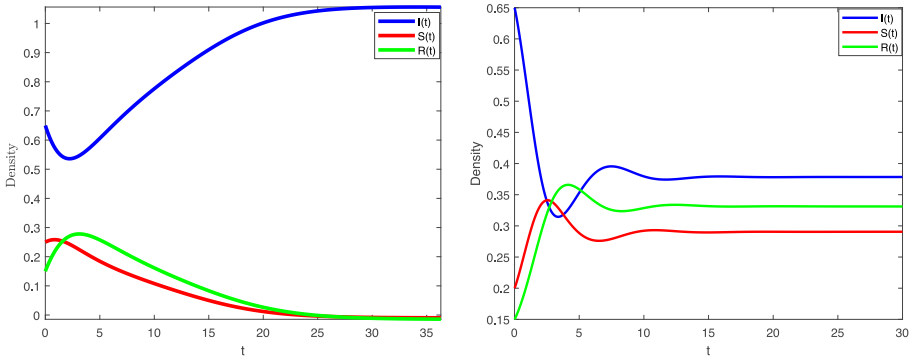

(a) (b)

Figure 3. The dynamical behavior of each state in model (2) without time delay.

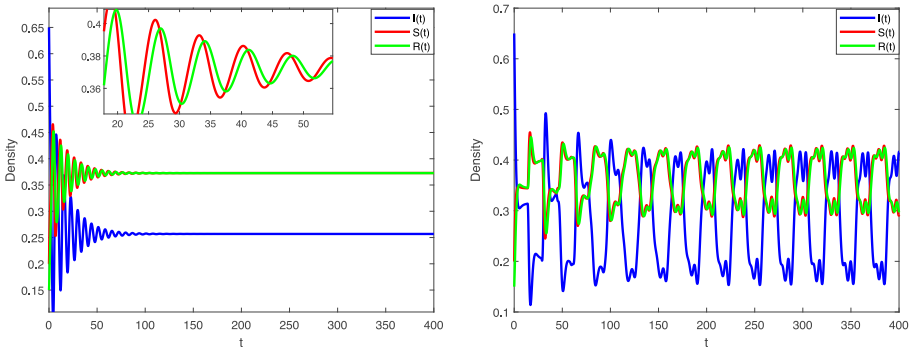

(a) (b)

Figure 4. The dynamical behavior of each state in model (5) when $\tau^1 \neq 0, \tau^2 = 0$.

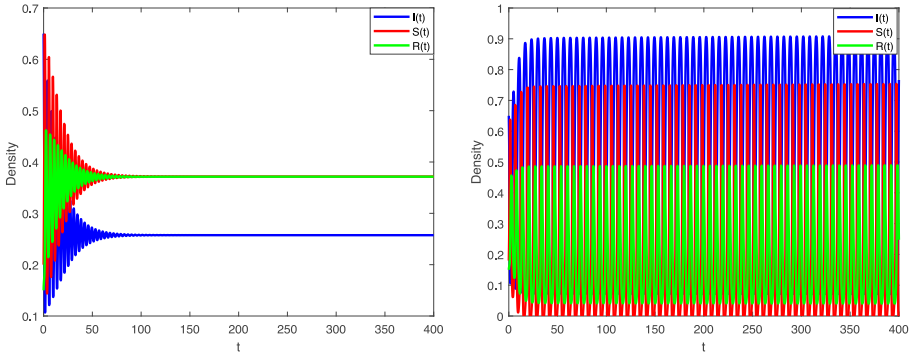

(a) (b)

Figure 5. The dynamical behavior of each state in model (5) when $\tau^2 \neq 0, \tau^1 = 0$.

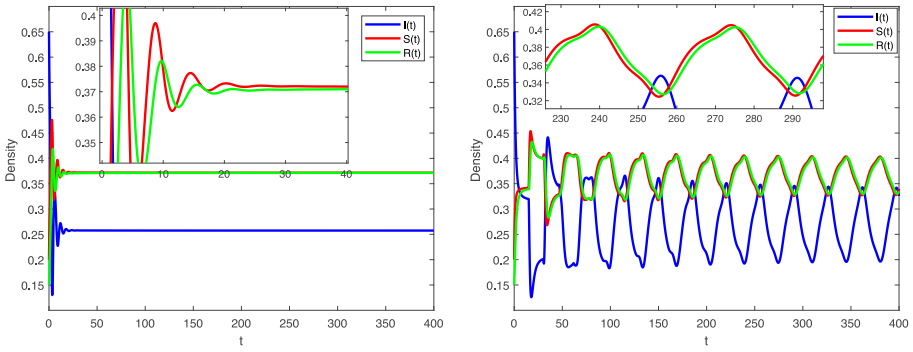

(a) (b)

Figure 6. The dynamical behavior of model (5) when $\tau^1 \neq 0$, $\tau^2 \in (0, \tau_{01}^2)$.

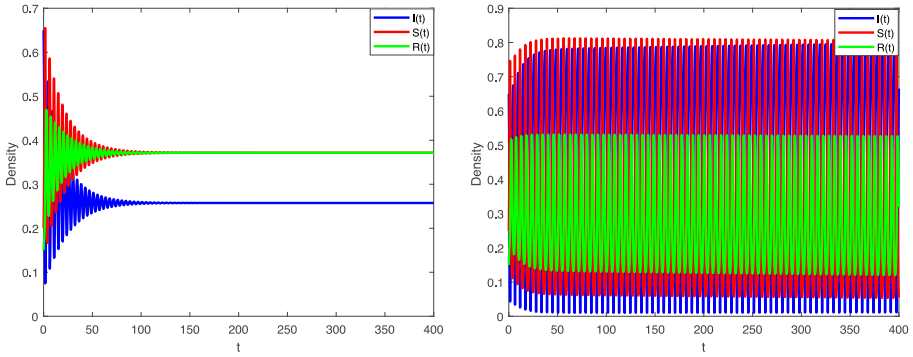

(a) (b)

Figure 7. The dynamical behavior of model (5) when $\tau^2 \neq 0$, $\tau^1 \in (0, \tau_{01}^1)$.

Example 5. Let $\tau^2 = 0.2 \in (0, \tau_{01}^2)$, $\tau^1 = 1 < \tau_{02}^1$ in Fig. 6(a) and $\tau^1 = 15 > \tau_{02}^1$ in Fig. 6(b). The values of other parameters are the same as in Example 4. According to Figs. 6(a) and 6(b), it can be drawn that the rumor-prevailing equilibrium E_1^* is locally asymptotically stable if $\tau^1 < \tau_{02}^1$ and $\tau^2 \in (0, \tau_{01}^2)$ and the rumor-prevailing equilibrium E_1^* is unstable if $\tau^1 > \tau_{02}^1$ and $\tau^2 \in (0, \tau_{01}^2)$. Therefore, there exists a Hopf bifurcation when τ^1 pass through τ_{02}^1.

Example 6. Let $\tau^1 = 0.2 \in (0, \tau_{01}^1)$, $\tau^2 = 0.68 < \tau_{02}^2$ in Fig. 7(a) and $\tau^2 = 0.75 > \tau_{02}^2$ in Fig. 7(b). The values of other parameters are the same as in Example 4. According to Figs. 7(a) and 7(b), it can be drawn that the rumor-prevailing equilibrium E_1^* is locally asymptotically stable if $\tau^2 < \tau_{02}^2$ and $\tau^1 \in (0, \tau_{02}^1)$ and the rumor-prevailing equilibrium E_1^* is unstable if $\tau^2 > \tau_{02}^2$ and $\tau^1 \in (0, \tau_{02}^1)$. Therefore, there exists a Hopf bifurcation when τ^2 pass through τ_{02}^2.

By comparing the solid and dashed lines of the same color in Fig. 8(a), we can observe that during the prevalence of rumors, the presence of higher-order interactions

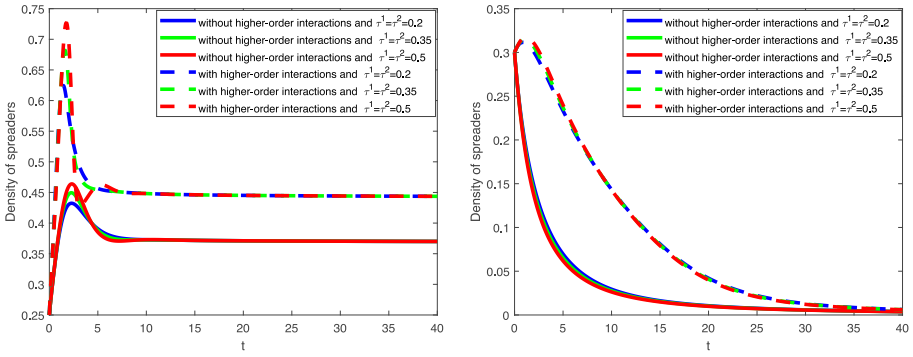

Figure 8. The effect of time delay and higher-order interactions on propagation.

leads to a higher peak and a broader spread in the propagation of rumors. Additionally, by comparing the solid and dashed lines of the same color in Fig. 8(b), we can see that during the decline of rumors, the existence of higher-order interactions significantly slows down the decay rate of the rumors. However, the influence of the presence or absence of higher-order interactions on the final disappearance time of the rumor is not obvious.

5 Model application

To better demonstrate the applicability of the model presented in this paper, in this section, we will select two real rumor cases from different domains for simulation and compare the performance differences between our model and other models in terms of simulation fitting.

5.1 Case 1: Crawfish rumor

In this part, we used as a data source the data collected on the website of Zhiwei about the "crawfish rumor", the main content of which is that initially, the doctor's analysis based on the patient's experience believed that the disease was related to eating crawfish, and then on May 3, 2018, a set of infected parasites and eggs caused by eating crawfish began to be widely disseminated. The "crayfish" rumor belongs to the public health field. The real data of this rumor are shown in Table 1, which is obtained from the propagation trend chart of Zhiwei website [7]. T is the unit time, N is the number of rumors forwarded.

Since rumors are usually initially posted by one or a few people, we let the initial value be $I(0) = 0.999$, $S(0) = 0.001$, $R(0) = 0$. Let $\langle k_\Delta \rangle = 3.9706$ and $\langle k \rangle = 4.5882$. Other parameters are chosen as $A = 0.048$, $d = 0.22$, $\xi_2 = 4$, $\eta = 0.445$, $\delta = 0.15$, $\sigma = 0.4$, $\tau^1 = \tau^2 = 0.1$. Using the data in Table 1 and the above parameter values, fit the model with actual data, and the results are revealed in Fig. 9. In Fig. 9, the rosy dashed line indicates the curve of the model of integer order, i.e., taking $\alpha = 1$; the blue dashed line indicates the curve of the model without considering higher-order interactions, i.e., taking

Table 1. The number of rumor spreader with time.

T	1d	2d	3d	4d	5d	6d	7d	8d	9d	10d
N	9	33	91	231	204	99	53	36	14	6
T	11d	12d	13d	14d	15d	16d	17d	18d	19d	20d
N	11	20	11	11	14	9	12	5	6	4

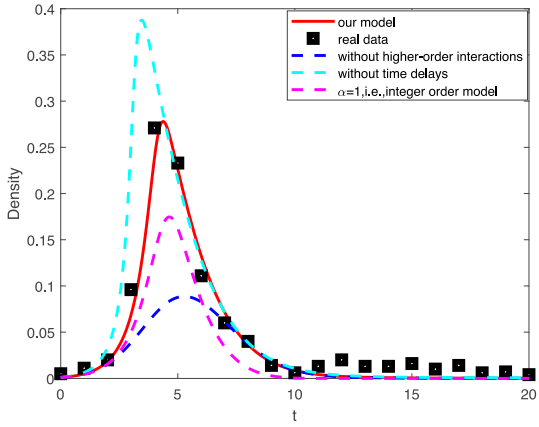

Figure 9. Fitting of the model to real datas.

$\xi_2 = 0$; the turquoise dashed line indicates the curve of the model without considering time delays, i.e., taking $\tau^1 = \tau^2 = 0$.

As seen from the red curve and blue dashed line in Fig. 9, higher-order interactions clearly contribute to the outbreak of rumors in the early stage, which better reflects the rapid outbreak and extinction of rumors and is more in line with reality. In contrast, the difference is minimal during the decline of the rumor, which is dominated by the recovery of the spreaders. The reason for this phenomenon is that we only consider higher-order interactions in the dissemination process but not in the recovery process. Because in our model, δ refers to the possibility of becoming a deleted individual due to losing interest or discovering the truth, representing the recovery process as spontaneous and active.

By comparing with the actual data, we should also justify the consideration of higher-order interactions in the propagation process only. By comparing the red solid line and turquoise dashed line in Fig. 9, it can be seen that time delay can effectively delay the speed and peak of rumor outbreak in the early stage, while the effect of time delay can be basically ignored in rumor decline stage.

Besides, a comparison of the red curve and the rosy dashed line in Fig. 9 shows that the fractional-order differential equation with the appropriate strength of memory effects is more responsive to the actual trend than the integer-order model in the early rumor, outbreak, and decline periods. To sum up, considering the effects of fractional derivatives, higher-order interactions, and time delays when modelling rumor propagation would be closer to the real rumor propagation trend.

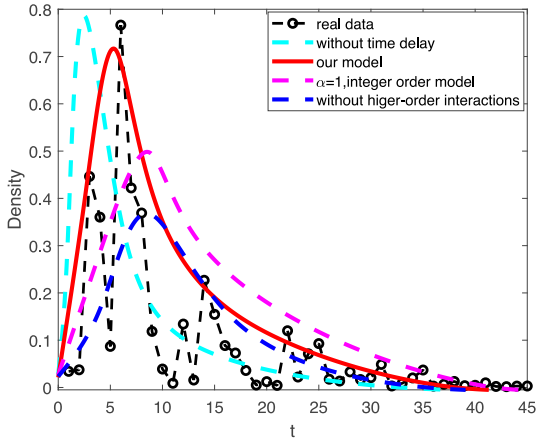

Figure 10. Fitting of the model to real datas.

5.2 Case 2: Elephants trample tourists

In this section, we select a rumor belonging to the field of public safety for model application. This rumor is called "Elephants Trampling Tourists", and the actual propagation data of this rumor comes from the research literature [27].

We set the initial values of the model as $I(0) = 0.973$, $S(0) = 0.027$, $R(0) = 0$. Referring to the model application section in reference [27], the values of other parameters of model (2) are set as $A = 0.048$, $d = 0.0675$, $\xi_2 = 2.8$, $\eta = 0.712$, $\delta = 0.185$, $\sigma = 0.12$, $\tau^1 = \tau^2 = 0.18$. Then we can obtain Fig. 10. From Fig. 10, it can be seen that the fitting effect of the proposed model remains the best. In addition, by comparing the different curves in Fig. 10, we can find that the existence of higher-order interactions and fractional derivatives enables the model to better characterize the peak value when the rumor breaks out; the addition of the time-delay factor can better predict the time when the rumor propagation reaches the peak.

Remark 11. Case 2 in this paper is the same as the case in the model application of reference [27]. We found that when $\alpha = 1$ in model (2), that is, it becomes an integer-order system, the obtained rosy dashed line is approximately similar to the fitting curve of the model in reference [27]. Both can reflect the general trend of real rumor propagation, but neither can accurately describe the peak situation of the rumor. When model (2) simultaneously considers time delay, higher-order interactions, and fractional derivatives, it can fit the real rumor propagation more accurately.

6 Conclusion

Practical significance. The proposed model provides a more detailed understanding of the way rumors spread, especially when higher-order interactions prevail. Such enhanced comprehension helps formulate more effective strategies to control rumors. For example,

we find that even if the threshold obtained by the next-generation matrix method is less than one, it cannot guarantee the disappearance of rumors. To this end, we need to adopt more precise and multidimensional prevention and control strategies. For instance, leveraging data analysis techniques, we should strive to identify potential risk points in higher-order interactions to stop rumors at their source. Additionally, in response to the group behavior effects that may occur during rumor propagation, we need to design flexible public opinion guidance mechanisms. For groups that are easily influenced by group polarization (such as the elderly and adolescents), we should provide them with diverse information and perspectives to help them form a more comprehensive and objective understanding.

Additionally, through the application of the model, we have found that the fractional-order rumor spreading model based on simplicial complexes exhibits enhanced performance in real-case simulations. This finding indicates that in the field of computer science, when predicting the spread of rumors, consideration should be given to higher-order interactions and fractional-order effects to enhance the accuracy of current prediction algorithms.

Theoretical significance. By combining fractional-order derivatives with higher-order interactions, this paper fills a crucial theoretical gap and enriches the modeling framework of rumor propagation. Using simplicial complexes to depict higher-order relationships provides researchers with an innovative approach. Notably, the revelation of bistability and the comprehensive exploration of Hopf bifurcation behavior under different conditions uncover the complex dynamic characteristics of rumor propagation. These findings offer new perspectives for the theoretical research on rumor propagation.

Future plans. We plan to deeply explore the role of higher-order interactions topology in rumor detection and tracing. Leveraging the current model's insights on the impact of higher-order interactions on rumor propagation dynamics, we will investigate using topological features like connectivity patterns and node centrality in simplicial complexes to create more efficient rumor source identification algorithms.

Author contributions. All authors have read and approved the published version of the manuscript.

References

1. E. Barrena, A. De-Los-Santos, J. Mesa, F. Perea, Analyzing connectivity in collective transportation line networks by means of hypergraphs, *Eur. Phys. J. Spec. Top.*, **215**:93–108, 2013, https://doi.org/10.1140/epjst/e2013-01717-3.

2. A. Bodo, G. Katona, P. Simon, SIS epidemic propagation on hypergraphs, *Bull. Math. Biol.*, **78**:713–735, 2016, https://doi.org/10.1007/s11538-016-0158-0.

3. G. Chen, C. Fan, J. Sun, J. Xia, Mean square exponential stability analysis for Itô stochastic systems with aperiodic sampling and multiple time-delays, *IEEE Trans. Autom. Control*, **67**:2473–2480, 2022, https://doi.org/10.1109/TAC.2021.3074848.

4. G. Chen, J. Xia, H. Ju, H. Shen, G. Zhuang, Sampled-data synchronization of stochastic Markovian jump neural networks with time-varying delay, *IEEE Trans. Neural Networks Learn. Syst.*, **33**:3829–3841, 2022, https://doi.org/10.1109/TNNLS.2021.3054615.
5. S. Chen, H. Jiang, L. Li, J. Li, Dynamical behaviors and optimal control of rumor propagation model with saturation incidence on heterogeneous networks, *Chaos Solitons Fractals*, **140**:110206, 2021, https://doi.org/10.1016/j.chaos.2020.110206.
6. D. Daley, D. Kendall, Stochastic rumours, *IMA J. Appl. Math.*, **1**:42–55, 1965, https://doi.org/10.1093/imamat/1.1.42.
7. Z. Date, Zhiwei data, 2021, https://ef.zhiweldata.com/eventOverview/bd599e638776c52b10003350.html.
8. P. Driessche, J. Watmough, Reproduction numbers and sub-threshold endemic equilibria for compartmental models of disease transmission, *Math. Biosci.*, **180**:29–48, 2002, https://doi.org/10.1016/s0025-5564(02)00108-6.
9. M. Girvan, M. Newman, Community structure in social and biological networks, *Proc. Natl. Acad. Sci. USA*, **99**:7821–7826, 2002, https://doi.org/10.1073/pnas.122653799.
10. H. Guo, X. Yan, Y. Niu, Event-triggered zero-gradient-sum distributed consensus optimization over directed networks, *J. Appl. Math. Comput.*, **69**:2473–2502, 2023, https://doi.org/10.1007/s12190-022-01829-5.
11. B. Jhun, M. Jo, B. Kahng, Simplicial SIS model in scale-free uniform hypergraph, *J. Stat. Mech. Theory Exp.*, **12**:123207, 2019, https://doi.org/10.1088/1742-5468/ab5367.
12. B. Li, L. Zhu, Turing instability analysis of a reaction-diffusion system for rumor propagation in continuous space and complex networks, *Inf. Process. Manage.*, **61**:103621, 2024, https://doi.org/10.1016/j.ipm.2023.103621.
13. Y. Moreno, M. Nekovee, A. Pacheco, Dynamics of rumor spreading in complex networks, *Phys. Rev. E*, **69**:066130, 2004, https://doi.org/10.1103/physreve.69.066130.
14. A. Nauman, R. Ali, R. Muhammad, Numerical and bifurcation analysis of SIQR model, *Chaos Solitons Fractals*, **150**:111133, 2021, https://doi.org/10.1016/j.chaos.2021.111133.
15. M. Nekovee, Y. Moreno, G. Bianconi, M. Marsili, Theory of rumour spreading in complex social networks, *Physica A*, **374**:457–470, 2007, https://doi.org/10.1016/j.physa.2006.07.017.
16. M. Newman, Finding community structure in networks using the eigenvectors of matrices, *Phys. Rev. E*, **74**:036104, 2006, https://doi.org/10.1103/physreve.74.036104.
17. Z. Pan, X. Wang, X. Li, Simulation investigation on rumor spreading on scale-free network with tunable clustering, *Int. J. Syst. Sci.*, **18**:2346–2348, 2006, https://doi.org/10.1360/jos172601.
18. H. Sha, L. Zhu, Dynamic analysis of pattern and optimal control research of rumor propagation model on different networks, *Inf. Process. Manage.*, **66**:104016, 2025, https://doi.org/10.1016/j.ipm.2024.104016.

19. P. Shu, Effects of memory on information spreading in complex networks, in *The 17th International Conference on Computational Science and Engineering, CSE 2014, 19–21 December 2014, Chengdu, China*, IEEE, Piscataway, NJ, 2014, pp. 554–556, https://doi.org/10.1109/CSE.2014.126.

20. J. Singh, A new analysis for fractional rumor spreading dynamical model in a social network with Mittag-Leffler law, *Chaos*, **29**:013137, 2019, https://doi.org/10.1063/1.5080691.

21. L. Xia, G. Jiang, Y. Song, B. Song, Modeling and analyzing the interaction between network rumors and authoritative information, *Entropy*, **17**:471–482, 2015, https://doi.org/10.3390/e17010471.

22. Y. Xia, H. Jiang, S. Yu, Z. Yu, The dynamic analysis of the rumor spreading and behavior diffusion model with higher-order interactions, *Commun. Nonlinear Sci. Numer. Simul.*, **138**:108186, 2024, https://doi.org/10.1016/j.cnsns.2024.108186.

23. Y. Xia, H. Jiang, Z. Yu, Global dynamics of ILSR rumor spreading model with general nonlinear spreading rate in multi-lingual environment, *Chaos Solitons Fractals*, **154**:111698, 2022, https://doi.org/10.1016/j.chaos.2021.111698.

24. Y. Xia, H. Jiang, Z. Yu, S. Yu, X. Luo, Dynamic analysis and optimal control of a reaction-diffusion rumor propagation model in multi-lingual environments, *J. Math. Anal. Appl.*, **331**:126967, 2022, https://doi.org/10.1016/j.jmaa.2022.126967.

25. D. Xiong, D. Liu, T. Li, M. Tian, Rumor spreading of a SEIR model in complex social networks with hesitating mechanism, *Adv. Difference Equ.*, **391**, 2018, https://doi.org/10.1186/s13662-018-1852-z.

26. M. Ye, J. Li, H. Jiang, Dynamic analysis and optimal control of a novel fractional-order 2I2SR rumor spreading model, *Nonlinear Anal. Model. Control*, **28**(5):859–882, 2023, https://doi.org/10.15388/namc.2023.28.32599.

27. S. Yu, Z. Yu, H. Jiang, S. Yang, The dynamics and control of 2I2SR rumor spreading models in multilingual online social networks, *Inf. Sci.*, **581**:18–41, 2021, https://doi.org/10.1016/j.ins.2021.08.096.

28. T. Yuan, G. Guan, S. Shen, L. Zhu, Stability analysis and optimal control of epidemic-like transmission model with nonlinear inhibition mechanism and time delay in both homogeneous and heterogeneous networks, *J. Math. Anal. Appl.*, **256**:127273, 2023, https://doi.org/10.1016/j.jmaa.2023.127273.

29. X. Yue, J. L. Huo, Analysis of the stability and optimal control strategy for an ISCR rumor propagation model with saturated incidence and time delay on a scale-free network, *Mathematics*, **69**:3900, 2022, https://doi.org/10.3390/math10203900.

30. Y. Zan, J. Wu, P. Li, SICR rumor spreading model in complex networks: counterattack and self resistance, *Physica A*, **405**:159–170, 2014, https://doi.org/10.1016/j.physa.2014.03.021.

31. D. Zanette, Criticality behavior of propagation on small-world networks, *Phys. Rev. E*, **64**:050901, 2001, https://doi.org/10.1103/physreve.64.050901.

32. Y. Zhang, J. Xu, A rumor spreading model considering the cumulative effects of memory, *Discrete Dyn. Nat. Soc.*, **2015**:1–11, 2015, https://doi.org/10.1155/2015/204395.

33. Y. Zhang, J. Xu, Y. Wu, A rumor control competition model considering intervention of the official rumor-refuting information, *Int. J. Mod. Phys. C*, **31**:205123, 2020, https://doi.org/10.1142/s0129183120501235.

34. L. Zhao, Q. Wang, J. Chen, Rumor spreading model with consideration of forgetting mechanism: A case of online blogging LiveJournal, *Physica A*, **390**:2619–2625, 2011, https://doi.org/10.1016/j.physa.2011.03.010.

35. G. Zhu, G. Jiang, L. Xia, Rumor spreading model considering conformity phenomena in complex social networks, *Comput. Sci.*, **43**:135–143, 2016, https://doi.org/10.11896/j.issn.1002-137X.2016.02.030.

36. L. Zhu, X. Zhou, Y. Li, Global dynamics analysis and control of a rumor spreading model in online social networks, *Physica A*, **526**:120903, 2019, https://doi.org/10.1016/j.physa.2019.04.139.